Position-dependent Lagrange interpolating multi-resolutions *

J. Baccou [a] and J. Liandrat [b]

[a] *LATP, Technopôle de Château-Gombert, 13451 Marseille Cedex 20, France*
E-mail: baccou@esm2.imt-mrs.fr
[b] *LATP and EGIM, Technopôle de Château-Gombert, 13451 Marseille Cedex 20, France*
E-mail: jliandrat@egim-mrs.fr

This paper is devoted to the construction of interpolating multi-resolutions using Lagrange polynomials and incorporating a position dependency. It uses the Harten's framework ([21]) and its connection to subdivision schemes. Convergence is first emphasized. Then, plugging the various ingredients into the wavelet multi-resolution analysis machinery, the construction leads to position-dependent interpolating bases and multi-scale decompositions that are useful in many instances where classical translation-invariant frameworks fail. A multivariate generalization is proposed and analyzed. We investigate applications to the reduction of the so-called Gibbs phenomenon for the approximation of locally discontinuous functions and to the improvement of the compression of locally discontinuous 1D signals. Some applications to image decomposition are finally presented.

Introduction

Even if the introduction of multi-scale approximations and corresponding wavelet bases has produced very efficient tools for the approximation/compression of functions and operators, essentially thanks to a nice mixing between localization in the spatial variable x and localization in the Fourier variable ω (see [13] for instance), non-optimal results are obtained when the analyzed element (function or operator) is locally non regular. This is very important in dimension larger than or equal to 2 and motivates a large number of recent works ([9], [12] or [25]). As an illustration, we consider in Figure 1 various approximations of the step function (Figure 1, top, left). The classical Gibbs phenomenon exhibited

* Research partially supported by European network "Breaking Complexity" #HPRN-CT-2002-00286

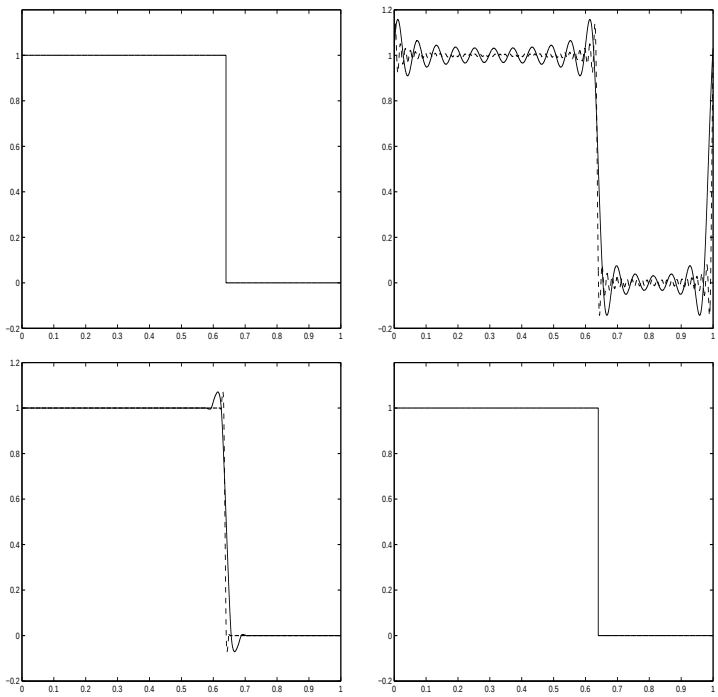

Figure 1. *Approximations of a step function, –: 2^5 interpolating points, ––: 2^7 interpolating points. From top, left to bottom, right: step function, spectral approximation (with periodic conditions), spline approximation, discontinuity-adapted approximation*

on Figure 1, top, right, occurs in the spectral approximation of this function (using Fourier interpolation) as well as in its spline interpolation (Figure 1, bottom, left). The multi-scale splitting of spline spaces and a standard adaptivity concept consisting, in this example, in selecting the N biggest coefficients of the decomposition of the step function on a classical spline wavelet basis, improves drastically the efficiency of the resulting reconstruction but locally the spurious oscillations typical of the Gibbs phenomenon remain.

The goal of this paper is to investigate one track to reduce such drawbacks by transforming the underlying approximation process used in the decomposition/reconstruction, taking into account the knowledge of the position of the singular points (in this example $x = 0.64$).

Taking apart the problem of singularity detection that is already addressed in many areas of signal processing ([10], [6]) and for which classical tools will be used in this paper, the key point in our investigations is then position-dependent multi-resolutions and wavelets.
Since it will become clear that a suitable setting to introduce position dependency is the Harten's multi-resolution ([21]), we start, in **Section 1**, by recalling the various definitions related to this framework. We particularly focus on the

connection between the Harten's framework incorporating a position dependency and non-stationary and non-uniform interpolating subdivision schemes. Convergence is then first emphasized since it is the key point for the existence of linear multi-resolutions.
Section 2 is devoted to the convergence analysis of univariate position-dependent interpolating subdivision schemes that are first specified. We completely analyze the case of position-dependent interpolating subdivision schemes associated to centered stencils.
In **Section 3** we provide a generalization to the bivariate case and its analysis.
In **section 4**, we present various applications. First, a result concerning the univariate Gibbs phenomenon is established. Then, the compression properties of position-dependent interpolating multi-resolutions are explored. Finally, some comparisons between our bi-variate generalization and a classical approach are performed in term of compression of a geometric image.

1. Harten's multi-resolution setting

A quick overview of Harten's setting is given in this section. More details can be found in [4] and [5].
In all the paper, $j \in \mathbb{Z}$ is a scale parameter, $k \in \mathbb{Z}$ is a position parameter and $x_k^j = k2^{-j}$ is referred as a dyadic real number belonging to the grid $X^j = \left\{x_k^j,\ k \in \mathbb{Z}\right\}$.

The general setting for Harten's multi-resolutions can be defined as a family of triplets $\left(V^j, D_j^{j-1}, P_{j-1}^j\right)$, $j \in \mathbb{Z}$ (see figure 2) where, for each j,

1. V^j is a separable space of approximation connected to a resolution level 2^{-j},
2. the operator D_j^{j-1} stands for a decimation operator from V^j onto V^{j-1} and
3. P_{j-1}^j, called a prediction operator, is a right inverse of D_j^{j-1} in V^{j-1}, i.e satisfies $D_j^{j-1}P_{j-1}^j = I_{V^{j-1}}$ where I_V is the identity in V.

It turns out to be that a suitable way to define the Harten's multi-resolution setting and the associated two-scale operators is to consider two other families of operators called discretization operators $\{D_j\}_{j\in\mathbb{Z}}$ and reconstruction operators $\{R_j\}_{j\in\mathbb{Z}}$. The discretization operators are supposed to be nested [1]. They form a family of linear operators that associate to any element f of a linear space F, a denumerable sequence $f^j = \left\{f_k^j\right\}_{k\in\mathbb{Z}} \in V^j = D_j(F)$. For each $j \in \mathbb{Z}$, the reconstruction operator R_j is a right inverse of D_j in V^j. It has not to be a linear operator.

It is easy to check that, with

[1] We say that $\{D_j\}_{j\in\mathbb{Z}}$ is nested if for all j and f, $D_j f = 0 \Rightarrow D_{j-1} f = 0$

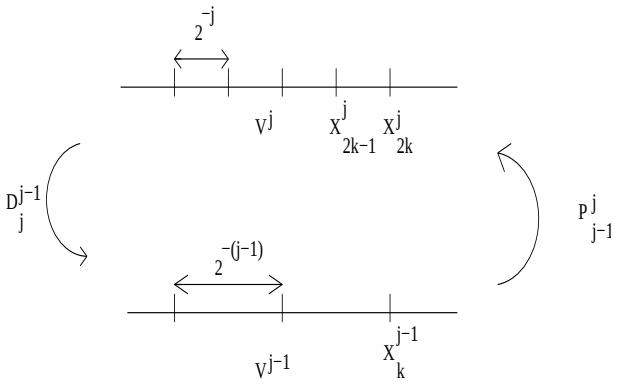

Figure 2. *Harten's multi-resolution*

$$P_{j-1}^{j} = D_j R_{j-1},$$
$$D_j^{j-1} = D_{j-1} R_j,$$

the family $\{\left(V^j, D_j^{j-1}, P_{j-1}^{j}\right)\}_{j\in\mathbb{Z}}$, defines a Harten's multi-resolution setting.

For any sequence $f^j \in V^j$, a sequence of detail coefficients $d^{j-1} = \left\{d_k^{j-1}\right\}_{k\in\mathbb{Z}}$ can be defined such that,

$$\forall k \in \mathbb{Z},\ d_k^{j-1} = f_k^j - \left(P_{j-1}^{j} f^{j-1}\right)_k. \tag{1}$$

Iterating this process, two multi-scale algorithms can be defined: the first one is a decomposition algorithm and reads, taking $j > J_0$,

$$f^j \mapsto \left\{f^{J_0}, d^{J_0}, ..., d^{j-1}\right\}, \tag{2}$$

while the second one is a reconstruction algorithm that reads, for $j > J_0$,

$$\left\{f^{J_0}, d^{J_0}, ..., d^{j-1}\right\} \mapsto f^j. \tag{3}$$

Remark 1.1.
Formulas (1), (2) and (3) establish the analogy between the Harten's framework and the classical wavelet setting ([13]). However, contrarily to the classical wavelet framework [2], in the Harten's setting, defining explicitly at each scale a re-

[2] where a prediction operator can be introduced using the filter associated to the chosen wavelet (see [7] for more details)

constructed function allows more flexibility for the construction of the prediction operator.

It will become clear in the next sections that this is a key point to improve the sparsity of the multi-scale representation when the data exhibit singularities.

The prediction operator P_{j-1}^{j} maps any element of V^{j-1} to an element of V^{j} and can therefore be interpreted as a subdivision scheme ([17]). More precisely, if we write:

$$\forall \{f_k^{j-1}\}_{k\in\mathbb{Z}} \in V^{j-1},\ \left(P_{j-1}^{j} f^{j-1}\right)_k = \sum_{m\in\mathbb{Z}} a_{k-2m}^{j,k} f_m^{j-1}, \tag{4}$$

then, the coefficients $\{a_m^{j,k}\}_{m\in\mathbb{Z}}$, $(j,k) \in \mathbb{Z}^2$, can be interpreted as the masks of a subdivision scheme. When $\{a_m^{j,k}\}_{m\in\mathbb{Z}}$ are independent of f^{j-1}, the subdivision scheme is said to be linear and moreover stationary (resp. uniform) if these coefficients do not depend on j (resp. on k).
In general, in the Harten's framework, P_{j-1}^{j} is not required to be a linear operator and therefore, the corresponding subdivision scheme is non-linear.

The multi-resolution algorithms (2) and (3) are known to be of great importance for data analysis and compression. In that framework, the notion of stability with regards to perturbations and the notion of convergence that are specified below are crucial.

Definition 1.1. Stability

The decomposition algorithm (2) is said to be stable with regards to the norm $||\ .\ ||$ if and only if,

$\exists C$ such that $\forall j,\ \forall (f^j, f_\epsilon^j)$, if $f^j \mapsto \left\{f^{J_0}, d^{J_0}, ..., d^{j-1}\right\}$ and $f_\epsilon^j \mapsto \left\{f_\epsilon^{J_0}, d_\epsilon^{J_0}, ..., d_\epsilon^{j-1}\right\}$, then,

$$||f_\epsilon^{J_0} - f^{J_0}|| \leq C||f_\epsilon^j - f^j||;\ \forall m < j,\ ||d_\epsilon^m - d^m|| \leq C||f_\epsilon^j - f^j||. \tag{5}$$

The reconstruction algorithm (3) is said to be stable with regards to the norm $||\ .\ ||$ if and only if,

$\exists C$ such that $\forall j > J_0, \forall \{f^{J_0}, d^{J_0}, ..., d^{j-1}\}$ and $\left\{f_\epsilon^{J_0}, d_\epsilon^{J_0}, ..., d_\epsilon^{j-1}\right\}$,
if $\{f^{J_0}, d^{J_0}, ..., d^{j-1}\} \mapsto f^j$ and $\left\{f_\epsilon^{J_0}, d_\epsilon^{J_0}, ..., d_\epsilon^{j-1}\right\} \mapsto f_\epsilon^j$, then,

$$||f_\epsilon^j - f^j|| \leq C\ sup\left(||f_\epsilon^{j-1} - f^{j-1}||, ||d_\epsilon^{j-1} - d^{j-1}||\right). \tag{6}$$

The convergence is related to the convergence of the subdivision schemes associated to P_{j-1}^{j}. Here, it is useful to define $\mathcal{C}(\mathbb{R})$ the space of functions f defined and continuous on $\mathbb{R}\backslash\mathcal{S}_f$ where $\mathcal{S}_f$ is a non-empty set of reals (depending of f) such that $\forall x \in \mathcal{S}_f, \lim_{y\to x, y>x} f(y) = f^+(x)$ and $\lim_{y\to x, y<x} f(y) = f^-(x)$ exist in $\mathbb{R}$ with $f^+(x) \neq f^-(x)$. We suppose moreover that the points of $\mathcal{S}_f$ are separated i.e

$$\exists \epsilon_{\mathcal{S}_f} > 0 \text{ such that } \forall x, y \in \mathcal{S}_f,\ x \neq y \Rightarrow |x-y| \geq \epsilon_{\mathcal{S}_f}.$$

We then propose the following definition:

Definition 1.2. Convergence of the subdivision scheme

The subdivision scheme associated to P_{j-1}^{j} is said to be L^∞-convergent if for any real sequence $\{f_k^0\}_{k\in\mathbb{Z}} \in V^0$, there exists a function $f \in \mathcal{C}(\mathbb{R})$ (called the limit function associated to f^0) such that:

$\forall \epsilon, \exists J$ such that $\forall j \geq J$ either

$$\| P_{j-1}^{j} ... P_1^2 P_0^1 f^0 - f^+\left(\frac{\cdot}{2^j}\right) \|_\infty \leq \epsilon, \tag{7}$$

or

$$\| P_{j-1}^{j} ... P_1^2 P_0^1 f^0 - f^-\left(\frac{\cdot}{2^j}\right) \|_\infty \leq \epsilon. \tag{8}$$

In general situations, there are few results on the stability or the convergence associated to algorithms (2) and (3). For linear algorithms, the convergence implies stability and when the associated subdivision scheme is stationary, the convergence analysis can be limited to the construction of functions, $\phi_m,\ m \in \mathbb{Z}$, defined for each m as the limit functions of the sequence $f_k^0 = \delta_{k,m},\ k \in \mathbb{Z}$.

In the following section, we focus on specific linear but position-dependent prediction operators and establish their convergence property.

2. Convergence analysis of Lagrange position-dependent subdivision schemes

2.1. Position-dependent prediction

From now on, the discretization operator D_j is the sampling operator defined by $\forall f \in \mathcal{C}(\mathbb{R})$, $(D_j f)_k = f^-\left(x_k^j\right)$.

Since the reconstruction operator is a right inverse of D_j in V^j, R_j is here an interpolation operator. Fixing once and for all a degree $D \geq 0$, the reconstruction considered here is the piecewise Lagrange polynomial interpolation of degree D defined for all $f^j \in V^j$ by,

$$R_j f^j(x) = \sum_{m=-l_{j+1,2k-1}}^{r_{j+1,2k-1}-1} L_m^{l_{j+1,2k-1},r_{j+1,2k-1}}(\frac{x - x_k^j}{2^{-j}}) f_{k+m}^j, \quad \text{if } x \in [x_{k-1}^j, x_k^j], \tag{9}$$

with,

$$L_m^{l_{j+1,2k-1},r_{j+1,2k-1}}(x) = \Pi_{n=-l_{j+1,2k-1},n\neq m}^{r_{j+1,2k-1}-1} \frac{x-n}{m-n}, \tag{10}$$

where $l_{j+1,2k-1}$ (resp. $r_{j+1,2k-1}$) denotes the number of left (resp. right) points in the interpolating stencil associated to the interval $[x_{k-1}^j, x_k^j]$ such that $l_{j+1,2k-1} + r_{j+1,2k-1} = D + 1$.

The prediction operator associated to this reconstruction is defined for all $k \in \mathbb{Z}$ as follows:

$$\begin{cases} f_{2k}^{\prime j} = \left(P_{j-1}^j f^{\prime j-1}\right)_{2k} = f_k^{\prime j-1}, \\ f_{2k-1}^{\prime j} = \left(P_{j-1}^j f^{\prime j-1}\right)_{2k-1} = \sum_{m=-l_{j,2k-1}}^{r_{j,2k-1}-1} L_m^{l_{j,2k-1},r_{j,2k-1}}(-1/2) f_{k+m}^{\prime j-1}, \end{cases} \tag{11}$$

with $\forall k \in \mathbb{Z},\ f_k^{\prime 0} = f_k^0$.

The associated subdivision scheme is defined by the following masks,

$$a^{j,2k} : \begin{cases} a_0^{j,2k} = 1, \\ a_m^{j,2k} = 0, \text{ for m} \neq 0, \end{cases} \tag{12}$$

and

$$a^{j,2k-1} : \begin{cases} a_{-2m-1}^{j,2k-1} = L_m^{l_{j,2k-1},r_{j,2k-1}}(-1/2) \text{ for } m = -l_{j,2k-1}, ..., r_{j,2k-1} - 1, \\ a_{2m}^{j,2k-1} = 0 \text{ otherwise.} \end{cases} \tag{13}$$

There are many interesting strategies to define the couple $(l_{j,2k-1}, r_{j,2k-1})$ according to the position $(2k-1)2^{-j}$.
A first one is $l_{j,2k-1} = l$, $r_{j,2k-1} = r$ (and thus $L_m^{l_{j,2k-1},r_{j,2k-1}} = L_m^{l,r}$) that leads

to **translation-invariant stencils**. The corresponding subdivision scheme is then stationary and uniform (and thus linear). When $l = r$, a direct correspondence between the interpolatory Harten's multi-scale framework (especially the prediction operator) and the interpolating subdivision scheme of Deslauriers and Dubuc (see [15]) can be exhibited.
A second strategy is $(l_{j,2k-1}, r_{j,2k-1})$ remaining functions of an a priori defined segmentation of the real line. It leads to **position dependent stencils** and defines a linear but non-stationary and non-uniform subdivision scheme.

To continue our investigations, we need to specify the position dependency of the stencil that we are interested in. It is motivated, as mentioned in the introduction by the approximation of piecewise smooth functions. We then propose the following definition of the stencil, associated to a family of separated segmentation points $\mathcal{S}_s$:

Definition 2.1. Position dependency

Given a family of segmentation points $\mathcal{S}_s$, a position-dependent stencil is controlled by:

- A triplet $(D, l, r),\ l > 0,\ r \geq 1$ and $l + r = D + 1$ such that $(l_{j,2k-1}, r_{j,2k-1}) = (l, r)$ when $[x^{j-1}_{-l+k}, x^{j-1}_{r-1+k}] \cap \mathcal{S}_s = \emptyset$.
- A rule for the selection of $(l_{j,2k-1}, r_{j,2k-1})$ when $[x^{j-1}_{-l+k}, x^{j-1}_{r-1+k}] \cap \mathcal{S}_s \neq \emptyset$.

Within this definition, the interpolating stencil is fixed by (l, r) at any point but in the vicinity of the segmentation points where the selection rule applies.
We end up this section by specifying a selection rule.

Since the segmentation points are separated, there exists a scale from which each segmentation point can be considered as isolated with regards to the stencil length. Therefore we focus in the following definition on a single segmentation point y_0 corresponding to $\mathcal{S}_s = \{y_0\}$.
The rule for the stencil selection is constructed in order to choose stencils that avoid the segmentation point y_0.
More precisely, given (D, l, r), the selection rule is defined as follows:

Definition 2.2. Stencil selection

Let us define for all $j \in \mathbb{Z}$, the index k_{j-1} s.t $y_0 \in [x^{j-1}_{k_{j-1}-1}, x^{j-1}_{k_{j-1}}]$. For all j and k such that $y_0 \in [x^{j-1}_{-l+k}, x^{j-1}_{r-1+k}]$, we set:

- If $y_0 \in [x^{j}_{2k_{j-1}-2}, x^{j}_{2k_{j-1}-1}[$, then

$S_{0,4}$	$\frac{35}{16}$	$-\frac{35}{16}$	$\frac{21}{16}$	$-\frac{5}{16}$
$S_{1,3}$	$\frac{5}{16}$	$\frac{15}{16}$	$-\frac{5}{16}$	$\frac{1}{16}$
$S_{2,2}$	$-\frac{1}{16}$	$\frac{9}{16}$	$\frac{9}{16}$	$-\frac{1}{16}$

Table 1
Lagrange coefficients associated to the stencil $S_{l,r}$

$$\begin{cases} \text{If } k < k_{j-1} \text{ then } r_{j,2k-1} = k_{j-1} - k \text{ and } l_{j,2k-1} = D + 1 - k_{j-1} + k, \\ \text{If } k \geq k_{j-1} \text{ then } r_{j,2k-1} = D + 1 + k_{j-1} - k \text{ and } l_{j,2k-1} = k - k_{j-1}. \end{cases} \tag{14}$$

- If $y_0 \in [x^j_{2k_{j-1}-1}, x^j_{2k_{j-1}}]$, then

$$\begin{cases} \text{If } k \leq k_{j-1} \text{ then } r_{j,2k-1} = k_{j-1} - k \text{ and } l_{j,2k-1} = D + 1 - k_{j-1} + k, \\ \text{If } k > k_{j-1} \text{ then } r_{j,2k-1} = D + 1 + k_{j-1} - k \text{ and } l_{j,2k-1} = k - k_{j-1}. \end{cases} \tag{15}$$

Figure 3, Table 1 and Figure 4 display this selection rule when $D = 3$, $l = 2$ and $r = 2$.

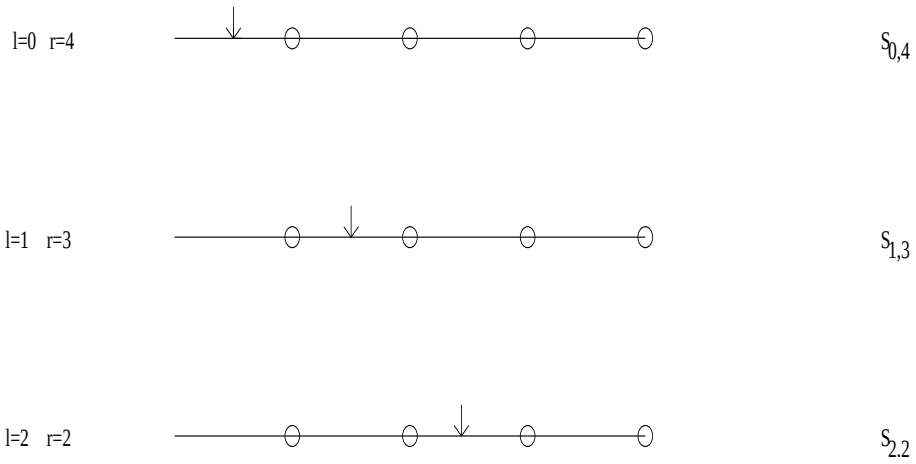

Figure 3. *Different stencils for 4-point interpolation associated to Definition 2.2. $S_{l,r}$ stands for the stencil with l left points and r right points.*

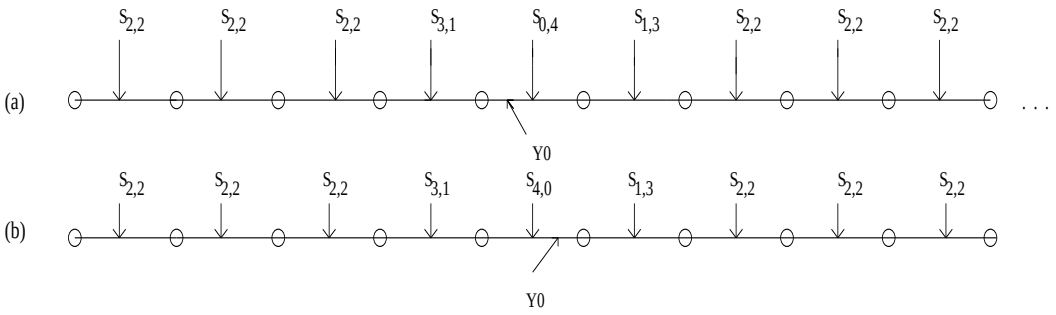

Figure 4. *Example of stencil selection following Definition 2.2. (a)* $y_0 \in [x^j_{2k_{j-1}-2}, x^j_{2k_{j-1}-1}]$, *(b)* $y_0 \in [x^j_{2k_{j-1}-1}, x^j_{2k_{j-1}}]$

Remark 2.1.
Note that Definition 2.2 and Figure 4 imply that if $f'^j_{2k_{j-1}-1}$ is located on the left (resp. on the right) of the segmentation point, the prediction operator coincides with extrapolation and non-centered interpolation (resp. non-centered and centered interpolations) for the two first predicted points on the left and with non-centered and centered interpolations (resp. extrapolation and non-centered interpolation) for the two first predicted points on the right.

2.2. Matrix formalism

There are many tools developed in the literature to study the convergence of linear subdivision schemes. In the case of uniform and stationary subdivision schemes, the Z-transform ([17]) or the Fourier transform ([13]) can be used. When translation invariance is lost (this is the case for position-dependent prediction operators), these approaches are useless. The matrix formalism, initially introduced in [24] and developed further in [19], [18] and [11] consists in deriving necessary and sufficient conditions for the convergence of a given subdivision scheme in terms of properties of matrices constructed from the masks of the subdivision scheme. More precisely, the convergence of the scheme is related to the convergence of infinite products of matrices belonging to a given set. The corresponding abstract problem is addressed in [14].

In our position-dependent subdivision scheme, according to Definition 2.1, it appears that, on one hand, for any point but segmentation points, the convergence is related to the convergence of the uniform and stationary interpolatory subdivision scheme associated to the Lagrange interpolation when the parameters of the stencil are (D, l, r). It therefore involves two so-called refinement matrices ([17]). On the other hand, for the segmentation points, the convergence analysis involves edge-matrices corresponding to the subdivision around segmentation points and depending on the position-dependency rule.

In the next section, we specify in the case of Definitions 2.1 and 2.2 the matrix formalism and the matrices introduced above and prove that they satisfy a sufficient property to ensure the convergence of our position-dependent subdivision scheme.

2.3. A general result of convergence

Following the previous section, two main situations must be considered: the uniform and stationary case for all regions far from the segmentation points and the edge case that takes place in the vicinity of segmentation points.

In the uniform and stationary case, we define following [17] F_k^j the minimal set of N points at level j that determines the values at dyadic points in the interval $[k2^{-j}, (k+1)2^{-j}]$ at level above j. The two $N \times N$ refinement matrices to be considered are the matrices A_0 and A_1 that transform the set F_k^j into the sets F_{2k}^{j+1} and F_{2k+1}^{j+1} as follows,

$$F_{2k}^{j+1} = A_0 F_k^j, \tag{16}$$

$$F_{2k+1}^{j+1} = A_1 F_k^j. \tag{17}$$

In the edge case, a simple generalization of the previous matrix formalism consists in considering, $\forall j \geq 0$, G_+^j (resp. G_-^j), the set of M points at level j that determines the corresponding points G_+^{j+1} (resp. G_-^{j+1}) in the right (resp. left) vicinity of y_0. Two $M \times M$-edge-matrices $A_{2,j}^+$ and $A_{2,j}^-$ are then defined by:

$$G_-^{j+1} = A_{2,j}^- G_-^j, \tag{18}$$

$$G_+^{j+1} = A_{2,j}^+ G_+^j. \tag{19}$$

Remark 2.2.
The dyadic procedure connected to the subdivision scheme implies that there always exists integers N and M such that the vectors F_k^j, G_-^j and G_+^j exist and consequently the matrices A_0, A_1, $A_{2,j}^+$ and $A_{2,j}^-$ can always be defined.

Remark 2.3.
By construction, our position-dependent subdivision scheme reproduces the polynomials up to degree D. Therefore, if $e = \{e_\beta\}_{0 \leq \beta \leq N-1}$ and $e' = \{e'_\beta\}_{0 \leq \beta \leq M-1}$, then $A_0 e = A_1 e = e$ and $A_{2,j}^+ e' = A_{2,j}^- e' = e'$.

Remark 2.4.
According to Definition 2.2, the matrices $A_{2,j}^+$ and $A_{2,j}^-$ depend on the binary development of the segmentation point y_0 and the set $\{A_{2,j}^+\}_{j \in \mathbb{Z}}$ (resp. $\{A_{2,j}^-\}_{j \in \mathbb{Z}}$) is reduced to a two-element set $\{A_{2,0}^+, A_{2,1}^+\}$ (resp. $\{A_{2,0}^-, A_{2,1}^-\}$) related to the

cases $y_0 \in [x^j_{2k_{j-1}-2}, x^j_{2k_{j-1}-1}[$ (System (14)) and $y_0 \in [x^j_{2k_{j-1}-1}, x^j_{2k_{j-1}}]$ (System (15)).

A convergence theorem of the position-dependent subdivision scheme follows from the matrix formalism.

We first introduce in the two following definitions some useful notations for the convergence theorem.

Definition 2.3.
If S is our position-dependent subdivision scheme and A_0, A_1 (resp. $A^+_{2,0}$, $A^+_{2,1}$, $A^-_{2,0}$ and $A^-_{2,1}$) are the corresponding refinement matrices (resp. edge-matrices), then, following [17],

there exists a subdivision scheme $\frac{1}{2}S_1^-$ (resp. $\frac{1}{2}S_1^+$) for the first difference $\delta f^j = \{\delta f^j_k\}_{k \le k_j - 2}$ (resp. $\delta f^j = \{\delta f^j_k\}_{k \ge k_j}$) with $\delta f^j_k = f^j_{k+1} - f^j_k$. It reads:

$$\forall k \le k_{j+1} - 2,\ \delta f^{j+1}_k = \frac{1}{2} S_1^-(\delta f^j)_k, \tag{20}$$

$$\forall k \ge k_{j+1},\ \delta f^{j+1}_k = \frac{1}{2} S_1^+(\delta f^j)_k. \tag{21}$$

We note $A^{(1)}_0$, $A^{(1)}_1$ (resp. $A^{(1),+}_{2,0}$, $A^{(1),+}_{2,1}$, $A^{(1),-}_{2,0}$ and $A^{(1),-}_{2,1}$) the refinement matrices (resp. the edge-matrices) associated to S_1^- and S_1^+.

Definition 2.4.
For any dyadic point $x = k_x 2^{-j_x}$, $x \neq y_0$, the differences $\delta f^j_{k2^{j-j_x}}$ and $\delta f^j_{k2^{j-j_x}-1}$, $j \ge j_x$ are computed according to the position of x through the levels. Three situations can occur:

1) the differences $\delta f^j_{k2^{j-j_x}}$ and $\delta f^j_{k2^{j-j_x}-1}$ are computed using the edge-matrices $A^{(1),+}_{2,i}$ if $x > y_0$ or $A^{(1),-}_{2,i}$ if $x < y_0$. We note $[j_x, j^0_x[$ the scale-range where this situation happens,

2) the differences $\delta f^j_{k2^{j-j_x}}$ and $\delta f^j_{k2^{j-j_x}-1}$ are computed using the refinement matrices $A^{(1)}_0$ or $A^{(1)}_2$. We note $]j^0_1, +\infty[$ the scale-range where this situation happens.

3) When $j \in [j^0_x, j^1_x]$, we say that the point x is in a transition zone.

Depending on the position of x, the interval $[j^0_x, j^1_x]$ may be empty as it is when $x = y_0$ or when x is far enough from y_0. For any x, we introduce $T_x = |j^1_x - j^0_x|$ with $T_x = 0$ when the interval is empty.

The following convergence theorem holds:

Theorem 2.1.
If there exists $L > 0$ such that,

$$\left(\frac{1}{2}\right)^L ||A_{i_1}^{(1)}....A_{i_L}^{(1)}||_\infty \leq \mu_0 < 1, \tag{22}$$

$$\left(\frac{1}{2}\right)^L ||A_{2,i_1}^{(1),-}....A_{2,i_L}^{(1),-}||_\infty \leq \mu_1 < 1, \tag{23}$$

$$\left(\frac{1}{2}\right)^L ||A_{2,i_1}^{(1),+}....A_{2,i_L}^{(1),+}||_\infty \leq \mu_2 < 1, \tag{24}$$

for all $(i_1, ..., i_L) \in \{0, 1\}^L$,

then the position-dependent subdivision scheme is punctually convergent.

Moreover, if there exists $T < \infty$ such that,

$$\forall x,\ T_x \leq T, \tag{25}$$

then the position-dependent subdivision scheme is uniformly convergent.

Proof:

The punctual convergence is a direct consequence of the fact that for any point x:

- either $x = y_0$ and the convergence on the right is a consequence of (24) and the convergence on the left is a consequence of (23),
- or $x \neq y_0$ and since after a finite number of iterations, the subdivision scheme is performed using the translation-invariant process, the convergence is a consequence of (22).

To get the uniform convergence, one must consider precisely the subdivision process at a fixed point $x = k_x 2^{-j_x}$, $x \neq y_0$. The only scales where the subdivision of the differences at the point x, $\delta f^j_{k2^{j-j_x}}$ and $\delta f^j_{k2^{j-j_x}-1}$, are not controlled by the edge and refinement matrices are $j_x^0 \leq j \leq j_x^1$. If $|j_x^1 - j_x^0|$ is uniformly bounded, since the masks of the subdivision scheme at these scales belong to a finite set independent of x, we get the uniform convergence.

■

In the next section, we provide the expression of the different matrices and their analysis in the case of the $D + 1$-point interpolating stencil.

2.4. Convergence analysis of the $D+1$-point position-dependent subdivision scheme with $l = r$

We start by specifying the subdivision scheme at non-segmentation points. The following proposition gives the expression of the two refinement matrices.

Proposition 2.1.
The two refinement matrices of the position-dependent subdivision scheme associated to the parameters (D, r, r) are the two $(4r-2)\times(4r-2)$-matrices defined as follows:

$$A_0 = \begin{bmatrix} 0 & \dots & \dots & 1 & 0 & \dots & \dots & \dots & \dots & \dots & 0 \\ L_{-r}^{r,r} & L_{-r+1}^{r,r} & \dots & L_{-1}^{r,r} & L_0^{r,r} & \dots & L_{r-1}^{r,r} & .. & \dots & \dots & 0 \\ 0 & \dots & \dots & \dots & 1 & 0 & \dots & \dots & \dots & \dots & 0 \\ 0 & \dots & \dots & \dots & \dots & \dots & \dots & \dots & \dots & \dots & \dots \\ \dots & \dots & \dots & \dots & \dots & \dots & \dots & \dots & \dots & \dots & \dots \\ \dots & \dots & \dots & \dots & \dots & \dots & \dots & \dots & \dots & \dots & \dots \\ \dots & \dots & \dots & \dots & \dots & \dots & \dots & \dots & \dots & \dots & \dots \\ \dots & \dots & \dots & \dots & \dots & \dots & \dots & \dots & \dots & \dots & \dots \\ \dots & \dots & \dots & \dots & \dots & \dots & \dots & \dots & \dots & \dots & \dots \\ 0 & \dots & \dots & \dots & \dots & \dots & \dots & \dots & L_{-r}^{r,r} & \dots & L_{r-1}^{r,r} \end{bmatrix},$$

and

$$A_1 = \begin{bmatrix} L_{-r}^{r,r} & \dots & L_0^{r,r} & \dots & L_{r-1}^{r,r} & \dots & \dots & \dots & \dots & \dots & 0 \\ 0 & \dots & 1 & 0 & \dots & \dots & \dots & \dots & \dots & \dots & 0 \\ 0 & \dots & \dots & \dots & \dots & \dots & \dots & \dots & \dots & \dots & \dots \\ \dots & \dots & \dots & \dots & \dots & \dots & \dots & \dots & \dots & \dots & \dots \\ \dots & \dots & \dots & \dots & \dots & \dots & \dots & \dots & \dots & \dots & \dots \\ \dots & \dots & \dots & \dots & \dots & \dots & \dots & \dots & \dots & \dots & \dots \\ \dots & \dots & \dots & \dots & \dots & \dots & \dots & \dots & \dots & \dots & \dots \\ \dots & \dots & \dots & \dots & \dots & \dots & \dots & \dots & \dots & \dots & \dots \\ \dots & \dots & \dots & \dots & \dots & \dots & \dots & \dots & \dots & \dots & \dots \\ 0 & \dots & \dots & \dots & \dots & \dots & L_{-r}^{r,r} & \dots & L_0^{r,r} & \dots & L_{r-1}^{r,r} \\ 0 & \dots & \dots & \dots & \dots & \dots & \dots & \dots & 1 & \dots & 0 \end{bmatrix}.$$

Moreover, their eigenvalues, except for the eigenvalue $\lambda_0 = 1$, are of modulus strictly less than 1.

Proof:

The expressions of A_0 and A_1 are taken from [17].
Since the convergence at non-segmentation points is equivalent to the convergence of the translation-invariant subdivision scheme with $l = r$, it results from [15] (i.e convergence of symmetric subdivision scheme) and from [17] (Theorem 4.2, p 67) that the eigenvalues of A_0 and A_1, except for $\lambda_0 = 1$, are of modulus strictly less than 1 .

■

Concerning the edge-matrices, as mentioned in Remark 2.4, their construction depends on the binary development of y_0. More precisely, the following proposition holds:

Proposition 2.2.
Writing for any $j \geq 0$, $y_0 \in [x^j_{k_j-1}, x^j_{k_j}]$, then, the vectors G^j_- and G^j_+ introduced in (18) and (19) are:

$$G^j_- = \{f^j_{k_j+\alpha}, \alpha = -2r, ..., -1\}, \tag{26}$$

$$G^j_+ = \{f^j_{k_j+\alpha}, \alpha = 0, ..., 2r-1\}. \tag{27}$$

Moreover, the four edge-matrices $A^-_{2,0}$, $A^-_{2,1}$, $A^+_{2,0}$ and $A^+_{2,1}$ are the $2r \times 2r$-matrices of the form,

- if $y_0 \in [x^{j+1}_{2k_j-2}, x^{j+1}_{2k_j-1}[$,

$$A^-_{2,0} = \begin{bmatrix} L^{r,r}_{-r} & ... & ... & L^{r,r}_0 & ... & L^{r,r}_{r-1} \\ 0 & ... & ... & 1 & 0 & ... \\ L^{r+1,r-1}_{-r-1} & ... & ... & ... & ... & L^{r+1,r-1}_{r-2} \\ ... & ... & ... & ... & ... & ... \\ ... & ... & ... & ... & ... & ... \\ L^{2r-1,1}_{-2r+1} & ... & ... & ... & ... & L^{2r-1,1}_0 \\ 0 & ... & ... & ... & ... & 1 \end{bmatrix},$$

$$A^+_{2,0} = \begin{bmatrix} L^{0,2r}_0 & ... & ... & ... & L^{0,2r}_{2r-1} \\ 1 & 0 & ... & ... & 0 \\ ... & ... & ... & ... & ... \\ ... & ... & ... & ... & ... \\ ... & ... & ... & ... & ... \\ L^{r-1,r+1}_{-r+1} & ... & L^{r-1,r+1}_0 & ... & L^{r-1,r+1}_r \\ ... & ... & 1 & ... & 0 \end{bmatrix}.$$

- if $y_0 \in [x_{2k_j-1}^{j+1}, x_{2k_j}^{j+1}]$

$$A_{2,1}^{-} = \begin{bmatrix} 0 & ... & 1 & 0 & ... \\ L_{-r-1}^{r+1,r-1} & ... & L_0^{r+1,r-1} & ... & L_{r-2}^{r+1,r-1} \\ ... & ... & ... & ... & ... \\ ... & ... & ... & ... & ... \\ 0 & ... & ... & ... & 1 \\ L_{-2r}^{2r,0} & ... & ... & ... & L_{-1}^{2r,0} \end{bmatrix},$$

$$A_{2,1}^{+} = \begin{bmatrix} 1 & 0 & ... & ... & ... & ... & 0 \\ L_{-1}^{1,2r-1} & ... & ... & ... & ... & ... & L_{1r-2}^{1,2r-1} \\ ... & ... & ... & ... & ... & ... & ... \\ ... & ... & ... & ... & ... & ... & ... \\ ... & ... & 1 & ... & ... & ... & 0 \\ L_{-r}^{r,r} & ... & L_0^{r,r} & ... & ... & ... & L_{r-1}^{r,r} \end{bmatrix}.$$

In both cases, $Sp(A_{2,i}^{+}) = Sp(A_{2,i}^{-}) = \{1, \frac{1}{2}, \frac{1}{2^2}, ..., \frac{1}{2^{2r-1}}\},\ 0 \leq i \leq 1.$

Proof:

The expressions of $A_{2,i}^{+}$ and $A_{2,i}^{-}$, $0 \leq i \leq 1$, are directly derived according to the stencil selection (Definition 2.2).
Moreover, since any $2r$-point Lagrange interpolation reproduces polynomials up to degree $2r-1$, their spectrum is $\{1, \frac{1}{2}, \frac{1}{2^2}, ..., \frac{1}{2^{2r-1}}\}$.

■

The following proposition that provides the uniform convergence applying Theorem 2.1 holds:

Proposition 2.3.
The refinement matrices (resp. edge-matrices) of the two subdivision schemes for the first difference satisfy the contraction properties of types (22)-(23)-(24). Moreover $|j_x^1 - j_x^0| \leq 2$.

Proof:

Following [17], the eigenvalues of $\frac{1}{2}A_0^{(1)}$ and $\frac{1}{2}A_1^{(1)}$ (resp. $\frac{1}{2}A_{2,i}^{(1),-}$ and $\frac{1}{2}A_{2,i}^{(1),+}$, $0 \leq i \leq 1$) are the eigenvalues of A_0 and A_1 (resp. $A_{2,i}^{-}$ and $A_{2,i}^{+}$, $0 \leq i \leq 1$) except $\lambda_0 = 1$. Therefore, according to Propositions 2.1 and 2.2, the spectral radius of the refinement matrices (resp. edge-matrices) of the two subdivision schemes for the first difference is strictly less than 1 and by norm equivalence,

there exists an integer, L, large enough to guarantee the contraction properties of types (22)-(23)-(24).

We now show that for any $x \neq y_0$, the transition scales (j_x^0, j_x^1) satisfy $|j_x^1 - j_x^0| \leq 2$.

Let us take $x > y_0$. On the right of y_0, the subdivision scheme is controlled by the matrices $A_{2,0}^+$, $A_{2,1}^+$, A_0 and A_1. We recall that the dimensions of these matrices are $2r \times 2r$ for $A_{2,0}^+$ and $A_{2,1}^+$ (Proposition 2.2) and $(4r-2) \times (4r-2)$ for A_0 and A_1 (Proposition 2.1). Therefore, $\frac{1}{2}A_{2,0}^{(1),+}$ and $\frac{1}{2}A_{2,1}^{(1),+}$ (resp. $\frac{1}{2}A_0^{(1)}$ and $\frac{1}{2}A_1^{(1)}$) are of size $(2r-1) \times (2r-1)$ (resp. $(4r-3) \times (4r-3)$).

It follows that the scales (j_x^0, j_x^1) satisfy $x \leq (2r-1)2^{-j_x^0}$ and $x \geq (4r-3)2^{-j_x^1}$. Therefore, $|j_x^1 - j_x^0| \leq 2$, that concludes the proof.

■

In what follows, we illustrate the convergence analysis introduced previously by detailing the case of the position-dependent subdivision scheme associated to $D = 3,\ l = 2,\ r = 2$ (Figure 3, Table 1 and Figure 4) that will be used in our applications.

Proposition 2.4.
When $l = r = 2$, the matrices involved in the convergence analysis are the following:

1) Refinement matrices:

$$A_0 = \begin{bmatrix} 0 & 1 & 0 & 0 & 0 & 0 \\ -\frac{1}{16} & \frac{9}{16} & \frac{9}{16} & -\frac{1}{16} & 0 & 0 \\ 0 & 0 & 1 & 0 & 0 & 0 \\ 0 & -\frac{1}{16} & \frac{9}{16} & \frac{9}{16} & -\frac{1}{16} & 0 \\ 0 & 0 & 0 & 1 & 0 & 0 \\ 0 & 0 & -\frac{1}{16} & \frac{9}{16} & \frac{9}{16} & -\frac{1}{16} \end{bmatrix}$$

and

$$A_1 = \begin{bmatrix} -\frac{1}{16} & \frac{9}{16} & \frac{9}{16} & -\frac{1}{16} & 0 & 0 \\ 0 & 0 & 1 & 0 & 0 & 0 \\ 0 & -\frac{1}{16} & \frac{9}{16} & \frac{9}{16} & -\frac{1}{16} & 0 \\ 0 & 0 & 0 & 1 & 0 & 0 \\ 0 & 0 & -\frac{1}{16} & \frac{9}{16} & \frac{9}{16} & -\frac{1}{16} \\ 0 & 0 & 0 & 0 & 1 & 0 \end{bmatrix}$$

with $Sp(A_0) = Sp(A_1) = \{1, \frac{1}{2}, \frac{1}{4}, \frac{1}{8}, -\frac{1}{16}\}$.

2) Edge-matrices:

$$A_{2,0}^{-} = \begin{bmatrix} -\frac{1}{16} & \frac{9}{16} & \frac{9}{16} & -\frac{1}{16} \\ 0 & 0 & 1 & 0 \\ \frac{1}{16} & -\frac{5}{16} & \frac{15}{16} & \frac{5}{16} \\ 0 & 0 & 0 & 1 \end{bmatrix}, \; A_{2,0}^{+} = \begin{bmatrix} \frac{35}{16} & -\frac{35}{16} & \frac{21}{16} & -\frac{5}{16} \\ 1 & 0 & 0 & 0 \\ \frac{5}{16} & \frac{15}{16} & -\frac{5}{16} & \frac{1}{16} \\ 0 & 1 & 0 & 0 \end{bmatrix},$$

and

$$A_{2,1}^{-} = \begin{bmatrix} 0 & 0 & 1 & 0 \\ \frac{1}{16} & -\frac{5}{16} & \frac{15}{16} & \frac{5}{16} \\ 0 & 0 & 0 & 1 \\ -\frac{5}{16} & \frac{21}{16} & -\frac{35}{16} & \frac{35}{16} \end{bmatrix}, \; A_{2,1}^{+} = \begin{bmatrix} 1 & 0 & 0 & 0 \\ \frac{5}{16} & \frac{15}{16} & -\frac{5}{16} & \frac{1}{16} \\ 0 & 1 & 0 & 0 \\ -\frac{1}{16} & \frac{9}{16} & \frac{9}{16} & -\frac{1}{16} \end{bmatrix}.$$

with $Sp(A_{2,i}^{+}) = Sp(A_{2,i}^{-}) = \{1, \frac{1}{2}, \frac{1}{4}, \frac{1}{8}\}, \; 0 \leq i \leq 1$.

Here, the contraction property can be established directly as:

$$\frac{1}{2}||A_{i_1}^{(1)}||_\infty < 1, \text{ for all } i \in \{0, 1\} \tag{28}$$

and

$$\left(\frac{1}{2}\right)^4 ||A_{2,i_1}^{(1),-} .... A_{2,i_4}^{(1),-}||_\infty < 1, \tag{29}$$

$$\left(\frac{1}{2}\right)^4 ||A_{2,i_1}^{(1),+} .... A_{2,i_4}^{(1),+}||_\infty < 1, \tag{30}$$

for all $(i_1, ..., i_4) \in \{0, 1\}^4$.

Some limit functions of the 4-point position-dependent subdivision scheme are plotted on Figure 5.

Remark 2.5.
- All the limit functions obtained in the previous construction are compactly supported since the position-dependent subdivision scheme uses masks of uniformly bounded length.
- Contrarily to the translation-invariant limit functions (see [4] for example), the position-dependent limit functions satisfy global scaling relation but are not separately refinable since the position-dependent subdivision scheme is non-uniform.

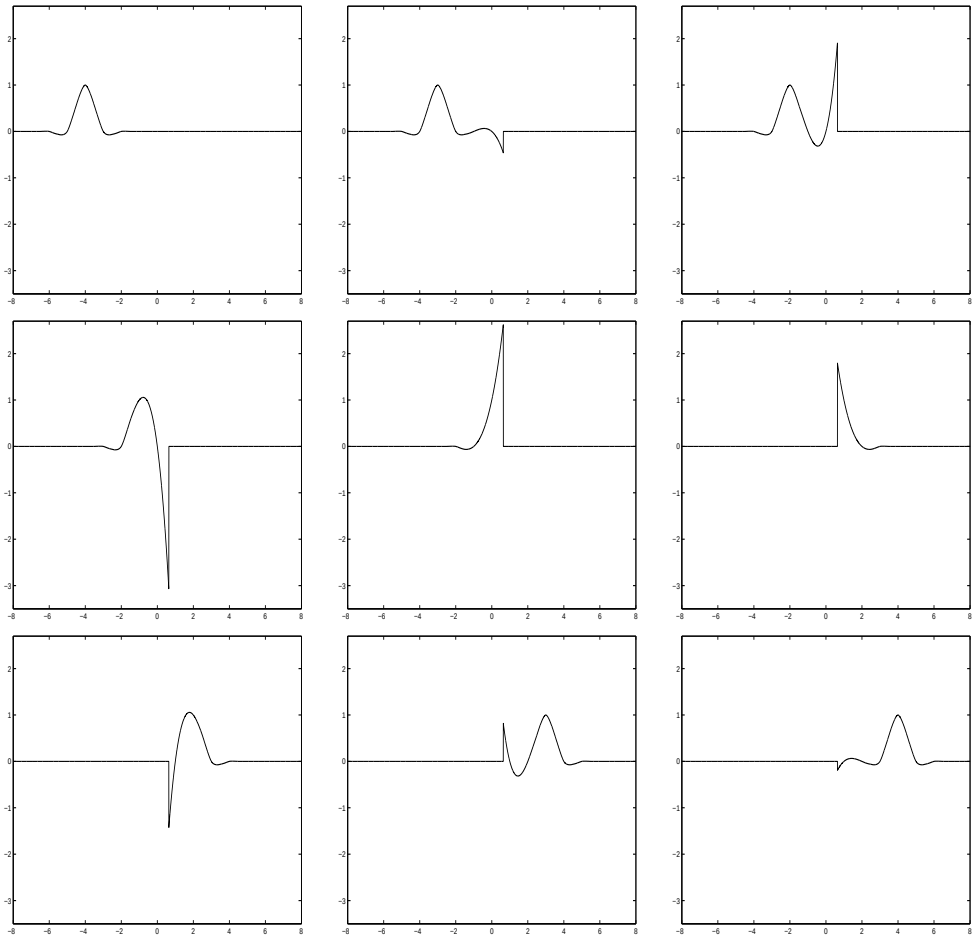

Figure 5. *Limit functions of the position-dependent subdivision scheme with* $D = 3,\ l = 2,\ r = 2$ *and* $y_0 = 0.64$. *From top left to bottom right,* $\phi_k,\ k = \{-4, -3, -2, -1, 0, 1, 2, 3, 4\}$.

Remark 2.6.
The analogy between the Harten's framework and the classical wavelet setting, already mentioned in Remark 1.1, can be now specified. It is possible to introduce a wavelet-like structure of the Harten's framework using the limit functions of the underlying subdivision schemes, $\{\phi_k\}_{k\in\mathbb{Z}}$. Following [4], one can introduce two families of spaces $\{V_j\}_{j\in\mathbb{Z}}$ and $\{W_j\}_{j\in\mathbb{Z}}$ such that,

$$V_j = span\left(\{\phi_k(2^j.)\}_{k\in\mathbb{Z}}\right), \tag{31}$$

$$W_j = span\left(\{\psi_k(2^j.)\}_{k\in\mathbb{Z}}\right), \tag{32}$$

where $\psi_k = \phi_{2k+1}$, that satisfy the classical properties of multi-resolution-

analysis spaces and detail spaces ([13], [22] or [23]).
Our construction can be interpreted as a generalization of the translation-invariant interpolating multi-resolution analyses described by Donoho in [16].
The main limitation of interpolating wavelets is their lack of vanishing moments. In order to circumvent this drawback, W. Sweldens in [26] introduced the so-called "lifting scheme". Another solution to construct position-dependent wavelets with more vanishing moments is to use a B-spline discretization operator . This construction has been described in [7] and [8].

3. 2D position-dependent subdivision schemes

We propose, here, a generalization of the previous position-dependent interpolating technique and of the associated multi-resolution to the bivariate case.
We first describe a 2D bi-directional position-dependent prediction. Then, we analyze the convergence of the corresponding subdivision scheme.

3.1. 2D bi-directional position-dependent prediction

Here, the segmentation points (Section 2.1) are generalized as a family $\mathcal{S}_s$ of continuous curves.
We formulate the following assumptions for the segmentation curves $\mathcal{S}_s$.

Definition 3.1.
Since it will be the case in the applications we have in mind, we assume for the rest of the paper that all the curves of $\mathcal{S}_s$ are defined as a reunion of vertical and/or horizontal segments which extremities are dyadic points of the form $(k2^{-J}, k'2^{-J})$ where J is a fixed level.

We assume moreover that they are separated i.e

$$\exists \epsilon_S, \text{ such that } \forall S_m, S_n \in S,\ \tilde{d}(S_m, S_n) \geq \epsilon_S,$$

where $\tilde{d}(A, B) = inf_{x \in A}\,(inf_{y \in B}|x - y|)$.
As in 1D, we can therefore focus on a single segmentation curve S_0.

To define the prediction operator, P^j_{j-1}, given a degree D, we consider at any level $j \geq J + log_2(D + 1)$ (see Remark 3.2) a splitting of the dyadic grid $X^j \times X^j$ into two zones (Figure 6, left) as follows:

$$Z_1 = \{(x, y) \in X^j \times X^j / d((x, y), S_0) < (D + 2)2^{-j}\}, \tag{33}$$

$$Z_2 = (X^j \times X^j) \backslash Z_1. \tag{34}$$

where $d\,((x, y), (x', y')) = sup\{|x-x'|, |y-y'|\}$ and $d\,((x, y), A) = inf\{d((x, y), (x', y')); (x', y') \in A\}$.

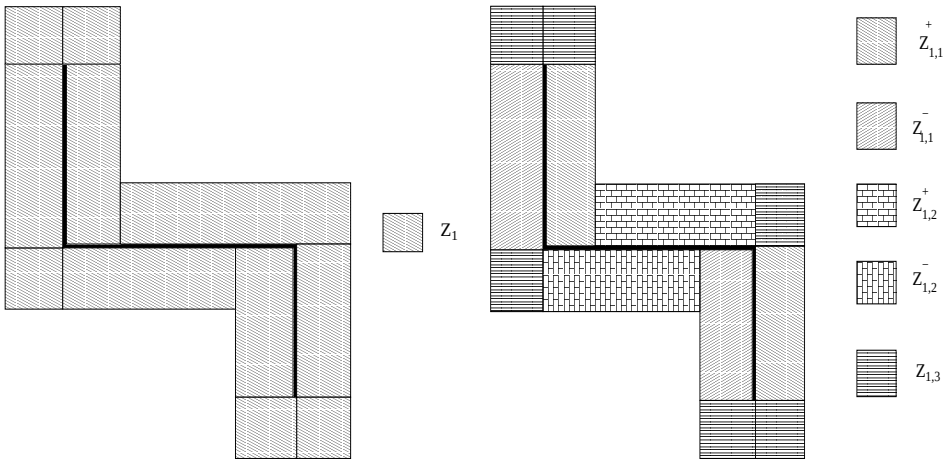

Figure 6. *Splitting of the dyadic grid in the vicinity of a segmentation curve S_0. The black line stands for S_0.*

Z_1 is called the boundary zone, it is then split into five zones, $Z^+_{1,1}$, $Z^-_{1,1}$, $Z^+_{1,2}$, $Z^-_{1,2}$ and $Z_{1,3}$ as can be seen on Figure 6, right.

Denoting a_Z, b_Z, c_Z and d_Z the upper, right, lower and left sides of a rectangle Z, we introduce the following notations that will be used in the sequel:

$$\mathcal{Z}^+_{1,1} = Z^+_{1,1} \backslash \{c_{Z^+_{1,1}}, d_{Z^+_{1,1}}\} \tag{35}$$

$$\mathcal{Z}^-_{1,1} = Z^-_{1,1} \backslash \{c_{Z^-_{1,1}}, d_{Z^-_{1,1}}\} \tag{36}$$

$$\mathcal{Z}^+_{1,2} = Z^+_{1,2} \backslash \{c_{Z^+_{1,2}}, d_{Z^+_{1,2}}\} \tag{37}$$

$$\mathcal{Z}^-_{1,2} = Z^-_{1,2} \backslash \{c_{Z^-_{1,2}}, d_{Z^-_{1,2}}\} \tag{38}$$

$$\mathcal{Z}_{1,3} = Z_{1,3} \backslash \{c_{Z_{1,3}}, d_{Z_{1,3}}\} \tag{39}$$

Remark 3.1.
For the sake of simplicity, the boundary zone and its different blocks have not been indexed by j. However, they are constructed at every level. In the sequel, we only specify the scale-index of a zone when necessary.

The prediction is constructed applying alternatively an univariate position-dependent prediction to the rows and to the columns of the data matrix. Therefore, it is called 2D bi-directional prediction.
More precisely, generalizing the notations of Section 2.1 to the 2D case, we start from an initial sequence $\{f^0_{m,n}\}_{(m,n)\in\mathbb{Z}}$ and introduce the following 2D interpolating prediction procedure,

$$\begin{cases} f'^{j+1}_{2m,2n} = f'^{j}_{m,n}, \\ \\ f'^{j+1}_{2m+1,2n} = \sum_{i=-l^H_{j+1,2m+1,2n}}^{r^H_{j+1,2m+1,2n}-1} L_i^{l^H_{j+1,2m+1,2n},r^H_{j+1,2m+1,2n}}(-1/2) f'^{j}_{m+i+1,n}, \\ \\ f'^{j+1}_{2m,2n+1} = \sum_{i=-l^V_{j+1,2m,2n+1}}^{r^V_{j+1,2m,2n+1}-1} L_i^{l^V_{j+1,2m,2n+1},r^V_{j+1,2m,2n+1}}(-1/2) f'^{j}_{m,n+i+1}, \\ \\ f'^{j+1}_{2m+1,2n+1} = \sum_{i=-l^V_{j+1,2m+1,2n+1}}^{r^V_{j+1,2m+1,2n+1}-1} L_i^{l^V_{j+1,2m+1,2n+1},r^V_{j+1,2m+1,2n+1}}(-1/2) f'^{j+1}_{2m+2i+2,2n+1}, \end{cases} \tag{40}$$

with $\forall (m,n) \in \mathbb{Z}^2$, $f'^{0}_{m,n} = f^0_{m,n}$ and where the superscript H (resp. V) refers to horizontal (resp. vertical) interpolating stencils. The stencil selection depends on the localization of the predicted point on the dyadic grid and especially on its membership of the block Z_2, $\mathcal{Z}^+_{1,1}$, $\mathcal{Z}^-_{1,1}$, $\mathcal{Z}^+_{1,2}$, $\mathcal{Z}^-_{1,2}$ or $\mathcal{Z}_{1,3}$.

The two following definitions specify the strategy in each block.

Definition 3.2. Prediction strategy in Z_2

The prediction in the block Z_2 coincides with the classical tensorial product of D+1-point translation-invariant univariate predictions ([1]).

Concerning the blocks in the boundary zone Z_1, the prediction operator at level $j+1$ is constructed in order to compute at level $j+1$ any blocks of type $\mathcal{Z}_{j+1}$ from the corresponding block, $\mathcal{Z}_j$ at level j.

Definition 3.3. Prediction strategy in $\mathcal{Z}^+_{1,1}$, $\mathcal{Z}^-_{1,1}$, $\mathcal{Z}^+_{1,2}$, $\mathcal{Z}^-_{1,2}$ and $\mathcal{Z}_{1,3}$

The stencil selection depends on the localization of the predicted point inside each block. We choose the following stencil:

- D+1-point centered stencil if all the points of the stencil are inside the block
- if not, the point to predict is located in the vicinity of the side of the block and we propose the following position-dependent treatment in the philosophy of the 1D-case (Remark 2.1):

1) Horizontal stencils: on the right of the side: extrapolation and non-centered interpolation, on the left of the side : non-centered and centered interpolations

2) Vertical stencils: above the side: extrapolation and non-centered interpolation, under the side: non-centered and centered interpolations

Remark 3.2.
In all the above definitions, we have assumed a connection between the prediction level j, the level J where the segmentation curve is defined and the degree D. This condition makes that Definition 3.3 is meaningful and that the different interpolations can indeed be evaluated in each block.

Remark 3.3.
This 2D prediction is position-dependent but the segmentation curve being assumed to be piecewise horizontal or vertical, the prediction directions are themselves horizontal or vertical. We refer to [7] or [3] for multi-directional predictions that incorporate more general directions.

In the next section, we analyze the convergence of the 2D bi-directional position-dependent prediction procedure defined by System (40), Definitions 3.2 and 3.3.

3.2. Convergence analysis

In the case of a tensorial product of univariate L^∞-convergent stationary and uniform subdivision scheme, the L^∞-convergence of the 2D procedure is straightforward.
When translation invariance is lost, because of the presence of segmentation curves, some extra-work is required to prove the convergence of the scheme.

Definition 3.4.
The convergence of the previously defined scheme occurs in the space $\mathcal{C}(I\!R^2)$ of functions f defined and continuous on $I\!R^2 \backslash \mathcal{S}_f$ where $\mathcal{S}_f$ is the family of segmentation curves satisfying Definition 3.1 associated to f.
On $\mathcal{S}_f$, for every point $X \in](k2^{-J}, k'2^{-J}); (k''2^{-J}, k'2^{-J})[\subset \mathcal{S}_f$, the limit $lim_{Y \to X, Y-X=\lambda n_X^+, \lambda>0} f(Y) = f^+(X)$ with n_X^+ a horizontal vector pointing to the right is assumed to exist as well as $lim_{Y \to X, Y-X=\lambda n_X^+, \lambda<0} f(Y) = f^-(X)$.
Similarly, on each interval of the type $](k2^{-J}, k'2^{-J}); (k2^{-J}, k''2^{-J})[\subset \mathcal{S}_f$, the limit $lim_{Y \to X, Y-X=\lambda n_X^+, \lambda>0} f(Y) = f^+(X)$ with n_X^+ a vertical vector pointing to the top is assumed to exist as well as $lim_{Y \to X, Y-X=\lambda n_X^+, \lambda<0} f(Y) = f^-(X)$.
On the vertices of $\mathcal{S}_f$, $X = (k2^{-J}, k'2^{-J})$, the function is assumed to have a limit on the top-right quarter plane called $f^+(X)$ as well as on the bottom-left quarter plane called $f^-(X)$.

On $\mathcal{C}(I\!R^2)$, the discretization operator D_j is the following sampling operator: if f is continuous at $(k2^{-j}, k'2^{-j})$, $(D_j f)_{k,k'} = f(k2^{-j}, k'2^{-j})$; if $(k2^{-j}, k'2^{-j}) \in \tilde{S}_f$, $(D_j f)_{k,k'} = f^-(k2^{-j}, k'2^{-j})$.

The generalization of Definition 1.2 is then:

Definition 3.5. Convergence of the 2D subdivision scheme

Given any family of segmentation curve $\mathcal{S}_s$, the subdivision scheme associated to the bi-variate prediction, P^j_{j-1} is said to be L^∞-convergent if for any real sequence $\left\{f^0_{m,n}\right\}_{(m,n)\in\mathbb{Z}^2}$, there exists a function $f \in \mathcal{C}(\mathbb{R}^2)$ with $\mathcal{S}_f = \mathcal{S}_s$ such that if f^+ and f^- stands for the two limits previously defined on $\mathcal{S}_f$ and $f^+(x,y) = f^-(x,y) = f(x,y)$ on $\mathbb{R}^2\backslash\mathcal{S}_f$,

$\forall\epsilon, \exists J$ s.t $\forall j \geq J$ either

$$\| P^j_{j-1}...P^2_1 P^1_0 f^0 - f^+\left(\frac{\cdot}{2^j}, \frac{\cdot}{2^j}\right) \|_\infty \leq \epsilon, \tag{41}$$

or

$$\| P^j_{j-1}...P^2_1 P^1_0 f^0 - f^-\left(\frac{\cdot}{2^j}, \frac{\cdot}{2^j}\right) \|_\infty \leq \epsilon. \tag{42}$$

We then have the following result:

Theorem 3.1.
The 2D position-dependent subdivision scheme is L^∞-convergent.

Proof:

By construction, for any point $X \in \mathbb{R}^2\backslash\mathcal{S}_s$, there exists a fixed level j_X (depending on the position of the point) such that, for every $j > j_X$, P^j_{j-1} coincides with the standard prediction associated to the tensorial product of translation-invariant predictions. Therefore, the punctual convergence is ensured in $\mathbb{R}^2\backslash\mathcal{S}_s$. On $\mathcal{S}_s$, the punctual convergence is also ensured because for any position, there exists a level from which P^j_{j-1} coincides with a tensorial product of 1D convergent predictions (involving the edge and refinement matrices introduced in Section 2.4).

As in the univariate case, the uniform convergence is also reached remarking that the thickness of the boundary zone Z_1 evolves with a factor $\frac{1}{2}$ at each scale. Therefore, any point outside of $\mathcal{S}_s$ is eventually in a transition zone during a fixed number of scales. Since for these scales, the subdivision masks belong to a finite set, the convergence is uniform. ∎

Remark 3.4.
Similarly to the 1D case, the limit functions of the underlying 2D bi-directional subdivision scheme can be interpreted as the scaling functions of a multi-

resolution analysis. It is then possible to introduce a 2D wavelet-like structure by constructing the corresponding wavelets. Two multi-scale transforms (one decomposition and one reconstruction) can also be constructed involving three sequences of detail coefficients.

4. Some applications and numerical tests

In this section, we investigate different situations that reveal the advantages of position dependent interpolating multi-resolution analysis for the approximation of univariate or bivariate locally discontinuous functions.

On one hand, it is known that when one approximates such functions, one has to face the so-called Gibbs phenomenon (see introduction and Figure 1). On the other hand, many efforts for the improvement of image compression algorithms concern the treatment of discontinuities.

4.1. The Gibbs phenomenon

We compare here the translation-invariant ([16]) and our position-dependent interpolating multi-resolution analysis with regard to the Gibbs phenomenon. More precisely, we analyze the approximations of the step function (defined by $f(x) = 1$ if $x \leq y_0$ and $f(x) = 0$ if $x > y_0$) (Figure 1, top, left) in the two sets of multi-resolution spaces where the stencil selection, in the position-dependent interpolating case, is performed using $\mathcal{S}_s = \{y_0\}$ as a unique segmentation point and Definitions 2.1 and 2.2 for the selection.

4.1.1. Translation-invariant multi-resolution

Let us call ϕ the unique limit (scaling) function used to define (by translation and dilation) the multi-resolution associated to the translation invariant prediction.

If the subdivision starts from the approximation $\left\{f_k^{J_0}\right\}_{k\in\mathbb{Z}} \in V^{J_0}$, $J_0 > 0$, then

$$\begin{cases} f_k^{J_0} = f\left(k2^{-J_0}\right) = 1 \text{ for } k \leq 0 \\ f_k^{J_0} = 0 \text{ for } k > 0. \end{cases}$$

The associated limit function f_{J_0}, also called the approximation of f at resolution J_0 is exactly

$$f_{J_0}(x) = \sum_{k\in\mathbb{Z}} f_k^{J_0}\phi\left(2^{J_0}x - k\right) = \sum_{k=-\infty}^{0} \phi\left(2^{J_0}x - k\right).$$

Because $\forall x \in I\!R$, $\sum_{k\in Z\!\!Z} \phi\left(2^{J_0}x - k\right) = 1$ ([16]) and $supp\,(\phi_0) = [(-2r + 1), (2l - 1)]$ ([15]) where *supp* stands for the support of a function, it is straightforward to prove that,

$$supp\left(\sum_{k=-\infty}^{0} \phi\left(2^{J_0}x - k\right) - f\right) \subset [(-2r + 2)2^{-J_0}, (2l - 1)2^{-J_0}], \qquad (43)$$

and therefore, the Gibbs phenomenon occurs on the interval $[(-2r + 2)2^{-J_0}, (2l-1)2^{-J_0}]$ as it can be observed on Figure 1, bottom, left where $D = 3$, $l = 2$ and $r = 2$.

4.1.2. Position-dependent interpolating multi-resolution

By construction, Definition 2.2 (Section 2.1) selects stencils that avoids the segmentation point y_0. Therefore, the oscillations due to the Gibbs phenomenon are completely removed as can be seen on Figure 1, bottom, right.

4.2. Compression of 1D-discontinuous signal

The Gibbs phenomenon is responsible for bad compression (in term of number of nonzero detail coefficients in the decomposition process) and/or bad reconstruction of signals around discontinuities. Therefore, according to the previous section, a position-dependent multi-resolution should lead to better compression and reconstruction. A complete discontinuity adapted multi-resolution has to couple a discontinuity detector and a position dependent multi-resolution. In addition to the Gibbs phenomenon previously investigated, the error in the segmentation/discontinuity points has also to be considered.

Note that the complete procedure (detection of discontinuities and position dependent analysis) provides a function-dependent (i.e non-linear) multi-resolution analysis comparable to the approach developed in [5], [1], [2] or [12].

In the sequel, we numerically investigate the effects of the influence of detection errors on the decomposition (Expression (2)) and reconstruction (Expression (3)) of a discontinuous function when using a position-dependent multi-resolution.

Two series of numerical tests are proposed. They provide a comparison between the position-dependent procedure (11) following Definitions 2.1 and 2.2, associated to the parameters $D = 4$, $l = 2$, $r = 2$, with a unique segmentation point $\mathcal{S}_s = \{y_0\}$ that we note (PD-4, y_0) and the translation-invariant multi-resolution associated to a centered-4-point stencil and noted TI-4.

The test function (Figure 7) is the following,

$$f(x) = 5\ sin\left(\pi(x - 0.1) + \frac{1}{6}\right)\chi_{]-\infty,0.64[} + \left(5 - 5\ sin\left(\pi(x - 0.1) + \frac{1}{6}\right)\right)\chi_{[0.64,+\infty[},$$

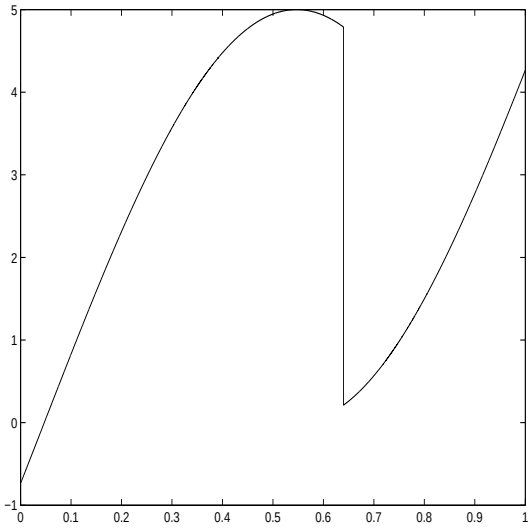

Figure 7. *Test function.*

(44)

with a discontinuity point at $x_0 = 0.64$.

The two series of tests follow the same track: the decomposition algorithm (2) is first applied to the discretized function, $\{f_k^{J_{max}}\}_{k\in\mathbb{Z}}$, providing the data $\{f^{J_0}, d^{J_0+1}, ..., d^{J_{max}}\}$. Then, after an ϵ-thresholding of the detail coefficients i.e,

$$\begin{cases} d_{\epsilon,k}^j = d_k^j \text{ if } \mid d_k^j \mid > \epsilon \\ d_{\epsilon,k}^j = 0 \text{ if } \mid d_k^j \mid \leq \epsilon \end{cases}$$

the reconstruction algorithm (3) is performed on the data $\{f^{J_0}, d_\epsilon^{J_0+1}, ..., d_\epsilon^{J_{max}}\}$ and leads to the reconstructed function, $f_\epsilon^{J_{max}}$.

- In the first series of tests, the segmentation point used to define the position-dependent prediction coincides exactly with the discontinuity of the function (i.e $y_0 = x_0 = 0.64$). According to our notations, we then compare (PD-4, 0.64) and TI-4.
- In the second series of tests, we assume that the segmentation point does not correspond perfectly with the discontinuity. We compare (PD-4, 0.641) and (PD-4, 0.665) corresponding to the segmentation points $y_0 = 0.641$ and $y_0 = 0.665$.

The performance of the decomposition is evaluated in term of nonzero detail coefficients (that we note nnz) remaining after thresholding. The precision

of the reconstruction is measured by the quality of the reconstructed function (evaluated as the discrete l^2-norm, $|| f^{J_{max}} - f_\epsilon^{J_{max}} ||_{l_2}$, for a given number of nonzero detail coefficients, nnz).

In all these tests, $J_0 = 4$ and $J_{max} = 13$.

Method	ϵ	Errors $\|\| f^{J_{max}} - f_\epsilon^{J_{max}} \|\|_{l_2}$	nnz
TI-4	$1e-6$	$5.6e-7$	67
	$1e-4$	$3.2e-5$	35
	$1e-3$	$9.5e-5$	27
	$1e-2$	$9.5e-5$	27
	1	$1.4e-1$	9
(PD-4,0)	$1e-6$	$5.8e-7$	48
	$1e-4$	$3.4e-5$	12
	$1e-3$	$1.5e-4$	1
	$1e-2$	$5.1e-4$	0
	1	$5.1e-4$	0

Table 2

Quality of the reconstruction in the translation-invariant (TI-4) and the position-dependent (PD-4,0) multi-resolutions.

Analysis of the results:

- From Table 2, it appears that with a perfect agreement between the segmentation point and the discontinuity, the position-dependent decomposition improves drastically the translation-invariant compression of the 1D-discontinuous signal. For an error remaining of the same order, the position dependent analysis provides a reduction of 50% or more on the number of non zero coefficients.

- When the stencil selection is performed using a non-fitted segmentation ($y_0 \neq 0.64$), a decay of the compression rate is noticeable (Tables 2 and 3) since more detail coefficients are kept. A strong disagreement between the discontinuity points and the segmentation points leads to a position-dependent scheme that behaves in terms of non-zero coefficients like the translation-invariant one. This result points out that an accurate localization of the discontinuity is essential to maintain the high performance of the compression.

Method	ϵ	Errors $\| f^{J_{max}} - f_\epsilon^{J_{max}} \|_{l_2}$	nnz
(PD-4,0.641)	$1e-6$	$5.5e-7$	65
	$1e-4$	$3.4e-5$	29
	$1e-3$	$1.4e-4$	19
	$1e-2$	$4.9e-4$	18
	1	$4.5e-2$	10
(PD-4,0.665)	$1e-6$	$6.6e-7$	68
	$1e-4$	$3.2e-5$	36
	$1e-3$	$1.6e-4$	25
	$1e-2$	$1.6e-4$	25
	1	$8.3e-2$	11

Table 3
Effect of a detection error on the quality of the position-dependent multi-resolution

4.3. Applications to image compression

We provide here an application of our 2D bi-directional position-dependent prediction procedure to image compression. Therefore, in all that follows, $(m,n) \in \{0,...,2^j-1\}^2$. Our motivation is the evaluation of the capabilities of the position-dependent approach keeping apart the problem of the determination of segmentation curves that refers to all the literature of edge detectors. Therefore, our tests are performed on a geometric image (see figure 8). It is not difficult to figure out that a simple detection using for instance the convolution of the original image with the Sobel operator ([20]) provides as segmentation curves the exact positions of the edges.

As in Section 4.2, the numerical tests focus on the quality of the decomposition and reconstruction steps incorporating the 2D position-dependent prediction. They provide a comparison between the position-dependent approach following Definitions 3.2 and 3.3 and associated to the parameters $D=3$, $l=2$, $r=2$, that we note **PD-4** , and the translation-invariant one based on the classical tensor product technique using a centered four point stencil (see [1]), that we note **TI-4**.

The performance of the decomposition process is evaluated, as in the 1D case, in term of nonzero detail coefficients remaining after thresholding (Table 4). The quality of the reconstruction step is evaluated through the "quality" of the reconstructed image for a fixed number of nonzero detail coefficients. The most usual way to measure this quality is to compute the $PSNR$ [3] (Table 4).

[3] By definition, $PSNR = 10\ log_{10}\left(\frac{256^2\ 2^{2J_{max}}}{||I^{J_{max}} - I_\epsilon^{J_{max}}||_{l^2}}\right)$

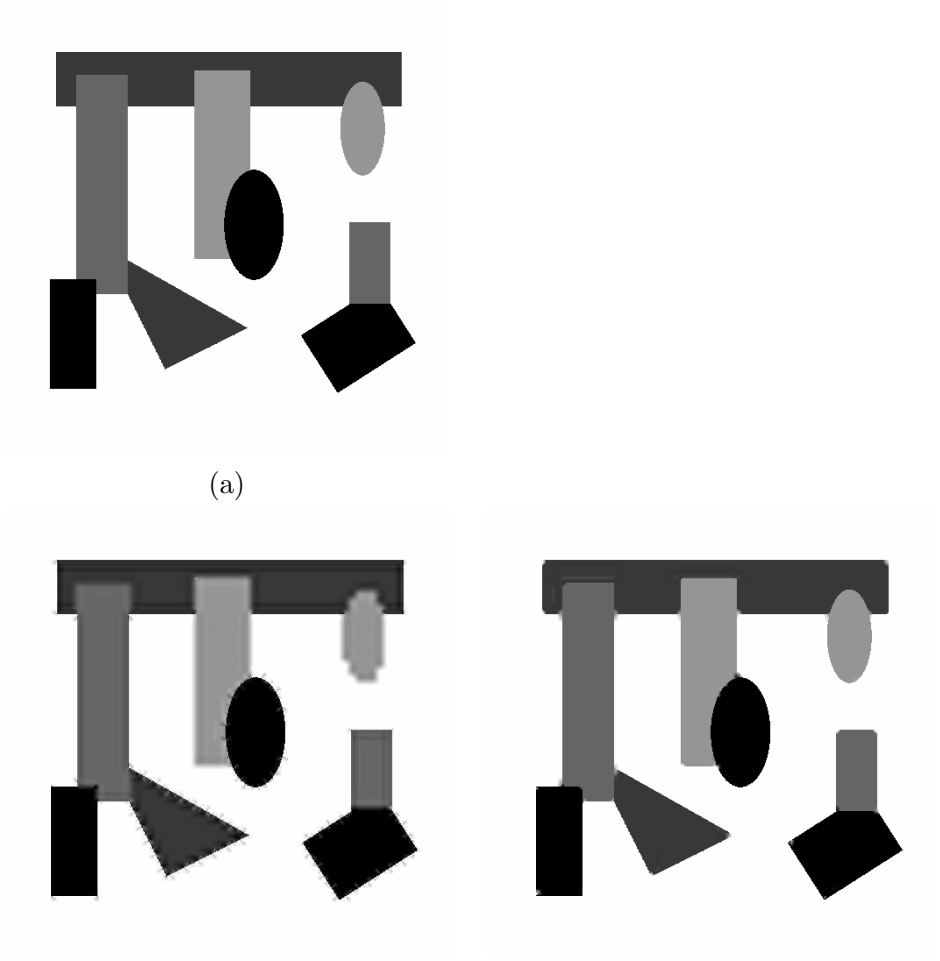

(a)

(b) (c)

Figure 8. *Reconstruction of a geometric image* $J_0 = 6$, $J_{max} = 9$. *(a) Original image, (b) Reconstructed image with a translation-invariant prediction (*$nnz = 4444$, $PSNR = 29.2$*), (c) Reconstructed image with a position-dependent prediction (*$nnz = 11$, $PSNR = 34.3$*).*

Note that the "visual quality" of the reconstructed image (Figure 8) is also an important criterium.

It comes out that the position-dependent prediction is very efficient. Indeed, for the same "quality" of image (in term of $PSNR$), the **PD-4** multi-resolution involves at least 100 times less nonzero detail coefficients than the **TI-4** multi-resolution (Table 4). The efficiency of the position-dependent strategy can also be observed, in term of "visual quality", on Figure 8, where it appears that very few detail coefficients are required to reduce the 2D Gibbs phenomenon around

Method	PSNR	nnz
PD-4	34.3	11
	42.9	111
	51	177
TI-4	33.8	7176
	40.7	13475
	50	18373

Table 4
"Reconstruction quality" of translation-invariant and position-dependent multi-resolutions

the edges.

Remark 4.1.
The numerical tests presented in this paper evaluate the efficiency of the position-dependent technique keeping apart the problem of edge detection. From these tests, It is clear that a position-dependent prediction involves far less nonzero detail coefficients to get a "good" reconstruction of image edges than when using a translation-invariant technique. However, for a perfectly fair comparison in term of compression of images, one should evaluate in each case the full memory storage required to store the compressed information. This memory storage is:
- in the translation-invariant case: the image on the coarsest grid X^{J_0} + the nonzero detail coefficients,
- in the position-dependent case: the image on the coarsest grid X^{J_0} + the nonzero detail coefficients + the family of segmentation curves.
The family of segmentation curves can be encoded as a binary matrix, therefore, much less bits are required for its encoding than for the detail coefficients encoding. Moreover, the encoding of the segmentation curves can be improved by using a chaining technique that basically consists in representing a curve as a starting point and a path (i.e a sequence of orientations) that describes the curve. These techniques as well as the coupling with edge detection are widely discussed in [3].

5. Conclusion

In this paper, a specific prediction operator in the framework of interpolatory Harten's setting has been defined and analyzed. It is oriented towards the representation of functions continuous everywhere but on specific sets of discontinuous points.
In 1D, given a family of segmentation points, a position-dependent prediction operator is indeed defined. Its convergence is established and allows the introduction of position-dependent scaling functions, wavelets and multi-resolution

algorithms.
A generalization to bi-variate situation is provided.
Applications in 1D configurations lead to the successful control of the classical Gibbs phenomenon associated to the approximation of locally discontinuous functions. Some encouraging results are provided for the compression of signals and images.

This approach can be considered as intermediate between the non-linear approaches defined and analyzed in [12], [5], [1] or [2] and the edge-adapted decompositions introduced for instance in [25].
The splitting between the singularity detection and the multi-resolution provides the advantage of the linearity and the stability of decompositions and reconstructions. The efficiency of this approach is being improved developing multi-directional predictions adapted to the normal direction of general edges. Efficient implementation for image compression involves sophisticated edge detectors and smart encoding for the segmentation curves as well as for the detail coefficients.

References

[1] S. Amat, F. Arandiga, A. Cohen, and R. Donat. Tensor product multiresolution analysis with error control for compact image representation. *Signal Processing*, 4:587–608, 2002.

[2] S. Amat, F. Arandiga, A. Cohen, R. Donat, G. Garcia, and M. von Oehsen. Data compression with ENO schemes: a case study. *Journal of Applied and Computational Harmonic Analysis*, 11:273–288, 2001.

[3] F. Arandiga, J. Baccou, M. Doblas, and J. Liandrat. Near-lossless image compression based on a multi-directional map-dependent algorithm. *ENUMATH Conference, Santiago de Compostela*, 2005.

[4] F. Arandiga, R. Donat, and A. Harten. Multiresolution based on weighted averages of the hat function I: linear reconstruction techniques. *SIAM J. Sci. Comput.*, 36(1):160–203, 1999.

[5] F. Arandiga, R. Donat, and A. Harten. Multiresolution based on weighted averages of the hat function II: non-linear reconstruction techniques. *SIAM J. Sci. Comput.*, 20(3):1053–1093, 1999.

[6] G. Aubert, M. Barlaud, O. Faugeras, and S. Jehan-Besson. Image segmentation using active contours: Calculus of variations or shape gradients. *SIAM Applied Mathematics*, 63(6):2128–2154, 2003.

[7] J. Baccou. *Analyses multirésolutions et problèmes de bords: applications au traitement d'images et à la résolution numérique d'équations aux dérivées partielles.* PhD thesis, Université d'Aix-Marseille I, LATP (Marseille), December 2004.

[8] J. Baccou and J. Liandrat. Position dependent multiresolutions and applications. *Proceeding of the Wavelet X conference, San Diego*, 2003.

[9] E.J Candès and D.L. Donoho. Curvelets - a surprisingly effective nonadaptive representation for objects with edges. *Curves and Surfaces, L. L. Schumaker et al. (eds), Vanderbilt*

University Press, Nashville, TN, 1999.

[10] V. Caselles, J.M. Morel, G. Sapiro, and A. Tannenbaum. Introduction to the special issue on partial differential equations and geometry-driven diffusion in image processing and analysis. *IEEE Trans. Image Proc.*, 7/3:269–273, 1998.

[11] A.S. Cavaretta, W. Dahmen, and C.A. Micchelli. Stationary subdivision. In *Memoirs of the American Mathematics Society*, volume 93 (453). Providence, Rhode Island, 1991.

[12] A. Cohen and B. Matei. Compact representations of images by edge adapted multiscale transforms. *IEEE ICIP conference, Tessaloniki*, 2001.

[13] I. Daubechies. *Ten lectures on wavelets*. SIAM, Philadelphia, 1992.

[14] I. Daubechies and J. Lagarias. Sets of matrices all infinite products of which converge. *Lin. Alg.and Appl*, 161:227–263, 1992.

[15] G. Deslauriers and S. Dubuc. Interpolation dyadique. In *Fractals, dimensions non entières et applications*, pages 44–45. Masson, Paris, 1987.

[16] D.L. Donoho. Interpolating wavelet transforms. *Technical report, Department of statistics, Stanford University*, 1992.

[17] N. Dyn. Subdivision schemes in computer-aided geometric design. In W.A Light, editor, *Advances in Numerical analysis II, Wavelets, Subdivision algorithms and Radial Basis functions*. Clarendon Press, Oxford, 1992.

[18] N. Dyn, J.A. Gregory, and D. Levin. A four-point interpolatory subdivision scheme for curve design. *Comp. Aid. Geom. Des.*, 4:257–268, 1987.

[19] N. Dyn, J.A. Gregory, and D. Levin. Analysis of linear binary subdivision schemes for curve design. *Constr. Appr. 7*, 2:127–148, 1991.

[20] R. Gonzalez and R. Woods. *Digital Image Processing*. Addison Wesley, 1992.

[21] A. Harten. Discrete multiresolution analysis and generalized wavelets. *J.of Applied Num.Math*, 12(3):153–193, 1993.

[22] S. Mallat. Multiresolution approximation and wavelets. *Trans Amer. Math. Soc.*, 315:69–88, 1989.

[23] Y. Meyer. *Ondelettes et Opérateurs I : Ondelettes*. Hermann, Paris, 1990.

[24] C.A. Miccheli and H. Prautzsch. Uniform refinement of curves. *Linear Algebra and Applications*, 114/115:841–870, 1989.

[25] E. Le Pennec and S. Mallat. Sparse geometrical image representations with bandelets. *IEEE Trans. on Image Processing*, 14(4):423–438, 2005.

[26] W. Sweldens. The lifting scheme: A construction of second generation wavelets. *SIAM J. Math. Anal.*, 29:511–546, 1997.